Surface Molecular Motion of Monodisperse α,ω-Diamino-Terminated and α,ω-Dicarboxy-Terminated Polystyrenes

Noriaki Satomi, Keiji Tanaka, Atsushi Takahara,† and Tisato Kajiyama*

Department of Applied Chemistry, Faculty of Engineering, Kyushu University, 6-10-1 Hakozaki, Higashi-ku, Fukuoka 812-8581, Japan

Takashi Ishizone and Seiichi Nakahama

Department of Polymer Chemistry, Faculty of Engineering, Tokyo Institute of Technology, 2-12-1 Ohokayama, Meguro-ku, Tokyo 152-8552, Japan

Received January 22, 2001; Revised Manuscript Received August 21, 2001

ABSTRACT: Surface glass transition behaviors of monodisperse α,ω-diamino-terminated and α,ω-dicarboxy-terminated polystyrenes (α,ω-PS$(NH_2)_2$ and α,ω-PS$(COOH)_2$) were studied by scanning force microscopy and were compared with the results of proton-terminated polystyrene (PS−H). All surface glass transition temperatures, T_g^s, of PS−H, α,ω-PS$(NH_2)_2$, and α,ω-PS$(COOH)_2$ were discernibly lower than each corresponding bulk glass transition temperature, T_g^b. However, the magnitude of T_g^s was strongly dependent on the chemical structure of chain end groups, because the surface concentration of chain ends varied with the surface free energy difference between the main chain part and the chain end portion, via the surface segregation or surface depletion of chain ends. This result makes it clear that chain end chemistry is one of determining factors on the magnitude of T_g^s. On the basis of the time−temperature superposition principle applied to the scanning rate dependence of lateral force as a function of temperature, the apparent activation energy, $\Delta H^{\ddagger}$, of the α_a-relaxation process corresponding to micro-Brownian motion at the surface was evaluated to be approximately 230 kJ mol^{-1}. This value is much smaller than the reported bulk ones and is independent of the chemical structure of chain ends. This result implies that the cooperativity for the α_a-relaxation process at the PS surface is reduced in comparison with the bulk, probably due to the existence of the free space presented to polymer segments at the surface. Hence, it was concluded that the surface α_a-relaxation process was activated by not only the chain end effect but also the reduced cooperativity at the surface. Finally, possible other factors determining on the magnitude of T_g^s were discussed.

Introduction

Glass transition and molecular mobility of polymer chains at the air/polymer interface have received a great deal of attention recently, due to importance in various functional applications such as permselective membranes, biomaterials, lubricants, adhesives, corrosion-resistant coatings, etc. Systematical understanding of surface properties, which are totally different from bulk ones, is crucial so that the performance of functional polymeric materials can be promisingly improved. This issue is also of pivotal importance and interest in the field as fundamentals of polymer science.

So far, many spectroscopic[1−4] and microscopic[5−9] methods have been applied to investigations of surface molecular motion. Jean et al. used Doppler broadening of energy spectra of positron annihilation coupled with a slow positron beam to reveal surface glass transition temperature, T_g^s, of polystyrene (PS). They showed that T_g^s was much lower than the bulk glass transition temperature, T_g^b, and asymptotically reached its bulk value with increasing distance from the outermost surface.[2] Liu et al. examined molecular mobility of rubbed PS films by the near-edge X-ray absorption fine structure (NEXAFS) dichroic ratio.[3] Since the dichroic ratio did not completely recover to zero below T_g^b, they concluded that molecular motion at the film surface was not activated in comparison with that in bulk. However, the dichroic ratio of NEXAFS started to decrease around 333 K. Hence, the molecular mobility at the PS surface seems to be enhanced in their experiment; otherwise, the dichroic ratio should remain to be the initial value. This is because the change in dichroic ratio corresponding to the change in the molecular orientation can be induced by a relatively large-scale molecular motion. Actually, Kerle et al. directly observed by atomic force microscopy (AFM) that an artificially rough PS surface started to flatten out even at a temperature below T_g^b.[10] Also, Schwab and co-workers, using optical birefringence of the rubbed PS surface, claimed that T_g^s was definitely lower than the corresponding T_g^b and chains closer to the surface relaxed more quickly than those in the bulk.[4] In addition, it has been demonstrated by several groups that surface chains can be dynamically moved even at a temperature below T_g^b.[11−13] Also, lower T_g in PS thin films can be rationalized based on a notion that T_g^s is lower than T_g^b.[14−17]

Since 1994, we have studied surface molecular motion of monodisperse proton-terminated PS (PS−H) films of approximately 200 nm thick, which is sufficient to avoid any ultrathining effects on surface molecular motion, based on scanning viscoelasticity microscopy (SVM) and lateral force microscopy (LFM), and concluded that T_g^s was much lower than T_g^b.[18−23] Although our consistent conclusion that surface molecular motion of the monodisperse PS−H is *activated* in comparison with the bulk has already emerged, it still opens why such active

* To whom correspondence should be addressed: Tel +81-92-642-3558; FAX +81-92-651-5606; E-mail kajiyama@cstf.kyushu-u.ac.jp.

† Present address: Institute for Fundamental Research of Organic Chemistry, Kyushu University.

10.1021/ma010126w CCC: $20.00
Published on Web 11/08/2001

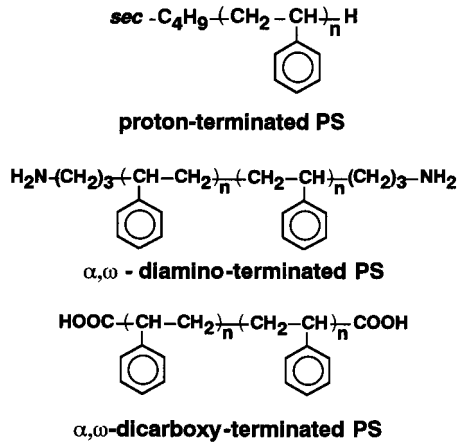

Figure 1. Chemical structures of PS−H, α,ω-PS$(NH_2)_2$, and α,ω-PS$(COOH)_2$.

Table 1. Characterizations of PSs Used in This Study

sample	M_n	M_w/M_n	T_g^b/K
PS−H	4.9K	1.09	354
	29K	1.08	374
	53K	1.03	377
	90K	1.05	378
	140K	1.05	382
	250K	1.03	382
	1,450K[a]	1.06	383
α,ω-PS$(NH_2)_2$	5.5K	1.25	358
	14K	1.07	374
	23K	1.08	374
	52K	1.08	377
	75K	1.12	378
α,ω-PS$(COOH)_2$[b]	5.1K	1.17	388
	12K	1.09	385
	52K	1.08	382
	94K	1.07	381

[a] Purchased from Pressure Chemical Co., Ltd. [b] Purchased from Polymer Source. Inc.

molecular motion takes place at the surface. For the moment, the authors have proposed the following reasons to rationalize it: end group effect[19,22] and reduced size and/or energy barrier of surface α_a-relaxation corresponding to micro-Brownian motion.[23] However, there still exist arguments that the chain end effect on activated surface molecular motion is trivial compared with the latter reason, namely, the reduced cooperativity at the surface.[24] If the chain end effect is one of responsible factors on surface molecular motion, the magnitude of T_g^s should be strongly dependent on what the chemical structure of chain end groups is. The objective of this study is to examine surface glass transition behaviors of monodisperse PSs with hydrophilic chain ends, which might be depleted at the film surface so as to minimize the air/polymer interfacial free energy.

Experimental Section

Materials and Film Preparation. Polymers used in this study were monodisperse PSs with various chain end groups, such as proton-terminated PS (PS−H), α,ω-diamino-terminated PS (α,ω-PS$(NH_2)_2$),[25] and α,ω-dicarboxy-terminated PS (α,ω-PS$(COOH)_2$). Figure 1 and Table 1 show the chemical structures and characterizations, respectively, of PS−H, α,ω-PS$(NH_2)_2$, and α,ω-PS$(COOH)_2$. Number-average molecular weight, M_n, and polydispersity, M_w/M_n, where M_w denotes weight-average molecular weight, were determined via gel permeation chromatography with PS standards. T_g^b was measured by differential scanning calorimetry (DSC). The monodisperse samples were used to avoid the influence of surface segregation of lower M_n components, due to smaller conformational entropy loss between surface and bulk, on surface molecular motion.

PS films for SVM and LFM measurements were coated from toluene solution onto cleaned silicon wafer with native oxide layer by a spin-coating method. The PS films were dried at room temperature for more than 24 h in air and then annealed at 423 K for 24 h in vacuo. The film thickness evaluated by ellipsometric measurement was approximately 200 nm, and an ultrathinning effect on surface properties was negligible in this thickness region.[26] AFM observation confirmed that the surface of these film was smooth enough for SVM and LFM measurements.

Scanning Force Microscopy (SFM). Glass transition behavior at PS surfaces with various chain ends was evaluated by using SFM (SPA 300HV with SPI 3800 controller, Seiko Instruments Industry Co., Ltd.). SVM and LFM measurements were carried out under vacuum in order to avoid surface oxidation and capillary force effect. The sample was heated with a heater located under the sample stage, and the surface temperature lower than room temperature was achieved by using liquid nitrogen. A piezoscanner was thermally insulated from the heating stage. The temperature calibration of the sample stage was carried out based on melting behavior of In and Ga on the sample stage, which was observed by a CCD camera. In or Ga was tightly fixed on the stage with the aid of Ag foil to attain a better thermal conductivity, and a thermocouple was precisely sandwiched between them. And then, the thermocouple was calibrated on the basis of the melting temperatures of In and Ga. In SFM measurements of PSs, a sample was similarly fixed by the Ag foil, and the temperature of the sample surface was always monitored by the thermocouple, which was sandwiched between the foil and the sample surface, during the measurement. A commercially available silicon nitride (Si_3N_4) tip on a rectangular cantilever with the bending spring constant of 0.12 ± 0.03 N m^{-1} (Olympus Co., Ltd.) was used. Both sides of the cantilever were coated with gold in order to reduce the temperature-induced bending of the cantilever due to the difference in the thermal expansion coefficients between Si_3N_4 and gold as small as possible. In the case of SVM measurement, the static normal force onto a cantilever tip was set to be 1 nN in a repulsive force region, and the frequency and amplitude of dynamic modulation at the supporting part of the cantilever were 4 kHz and 1 nm, respectively. For LFM measurement, the normal force onto the tip was fixed to be 10 nN, and the scanning rate was varied from 10^2 to 10^5 nm s^{-1}. Although the tip indentation depth is not necessarily the same in both measurements, we assume for the moment that both analytical depths are not so different. The dependence of T_g^s on the static normal force and the dynamic modulation amplitude for SVM measurement will be reported shortly.[27] It was preconfirmed that the film surface was not damaged after SVM and LFM measurements.

X-ray Photoelectron Spectroscopy (XPS). To examine surface concentration of chain end groups of α,ω-PS$(NH_2)_2$, XPS measurement was carried out. The XPS spectra were obtained with a Phi ESCA 5800 X-ray photoelectron spectrometer (Physical Electronics Co., Ltd.) at 293 K. The X-ray source was monochromatic Al Kα X-ray operated at 14 kV and 25 mA. The N_{1s} spectrum was calibrated based on the binding energy of 285.0 eV for neutral carbon.

Results and Discussion

Determination of Surface Glass Transition Temperature by SVM. To evaluate T_g^s for the monodisperse PS with various chain termini, the surface phase lag, δ^s, between imposed stimulus displacement signal and detected response force one was measured by SVM. The absolute value of δ^s has not been successfully obtained at present because of the difficulty in the determination of a calibration constant of mechanical vibration system.[19] Thus, the relative change of δ^s was examined as a function of temperature for each PS film.

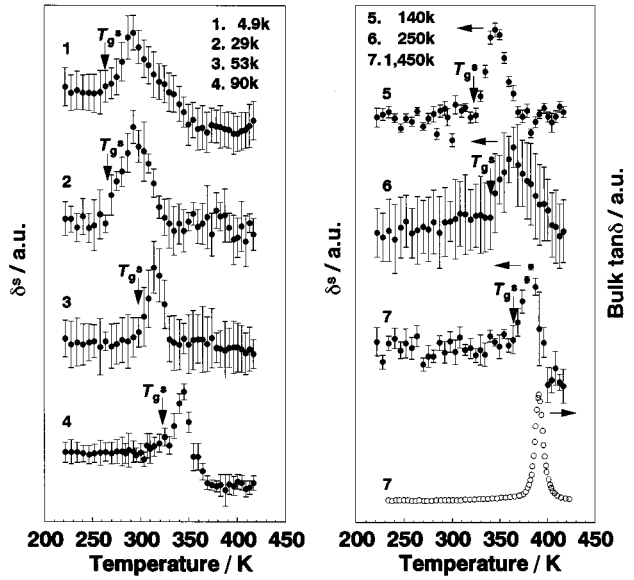

Figure 2. Temperature dependence of δ^s for the monodisperse PS−H films with M_n of 4.9K to 1450K by SVM. The bulk tan δ measured by Rheovibron for the PS−H film with M_n of 1450K are shown by the open circles.

Figure 2 shows the temperature dependence of δ^s for the PS−H films with M_n of 4.9K to 1450K. For a comparison, the bulk mechanical loss tangent, tan δ, of PS−H with M_n of 1450K was also plotted in it. The bulk tan δ was measured as a function of temperature by Rheovibron (DDV-01FP, Orientec A&D Co., Ltd.) at 3.5 Hz. A peak observed in Figure 2 can be assigned to the α_a-relaxation at the surface[20] or in the bulk,[28] and it is clear that the δ^s peak appears in a lower temperature region compared with that of the bulk tan δ peak. Since the measuring frequencies of our SVM and Rheovibron are 4 kHz and 3.5 Hz, respectively, the peak temperature difference between δ^s and bulk tan δ should be increased if Rheovibron is operated at the same frequency as SVM, 4 kHz. Thus, it seems reasonable to claim that the glass−rubber transition at the surface takes place in a lower temperature range than that in the bulk.

Surface molecular motion of PS terminated by different end groups from *sec*-butyl group and proton-terminated repeating unit has not been studied yet. Hence, SVM measurements of α,ω-PS$(NH_2)_2$ and α,ω-PS$(COOH)_2$, which had *hydrophilic* end groups compared with the main-chain part, were made to examine T_g^s. Figures 3 and 4 show the temperature dependence of δ^s as a function of M_n for the α,ω-PS$(NH_2)_2$ and α,ω-PS$(COOH)_2$ films, respectively. Similarly, the peak corresponding to the surface micro-Brownian motion was apparently observed on each δ^s−temperature curve. An onset temperature, at which the magnitude of δ^s starts to increase, can be empirically defined as T_g^s,[29] and T_g^ss so determined are marked by the arrows in Figures 2−4.

Figure 5 shows the M_n dependences of T_g^s and T_g^b for the PS−H, α,ω-PS$(NH_2)_2$, and α,ω-PS$(COOH)_2$ films. T_g^b was measured by DSC. As a general trend, T_g^s was lower than the corresponding T_g^b. This result makes it clear that thermal molecular motion at the surface is more active than that in the bulk, independent of chain end chemistry. However, the magnitude of T_g^s was strongly dependent on the chain end species at a given M_n. Hence, it is clear that the chain end effect is one of the responsible determining factors on the magnitude of T_g^s.

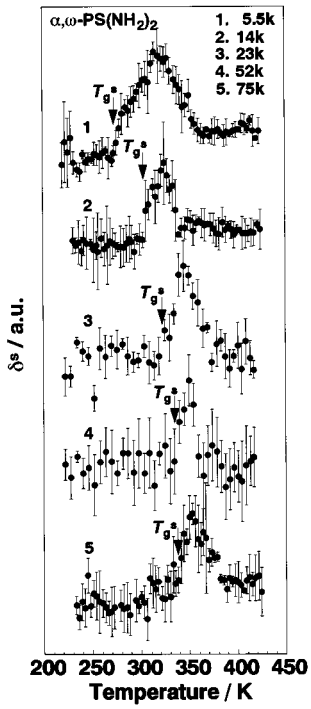

Figure 3. Temperature dependence of δ^s for the monodisperse α,ω-PS$(NH_2)_2$ films with M_n of (1) 5.5K, (2) 14K, (3) 23K, (4) 52K, and (5) 75K.

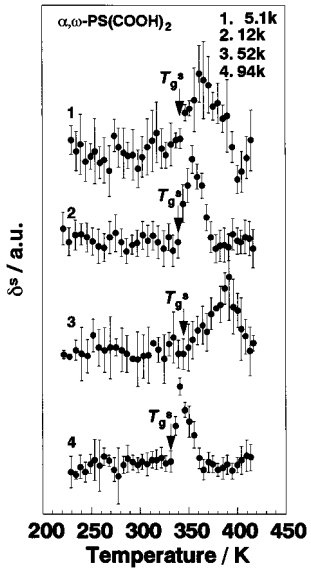

Figure 4. Temperature dependence of δ^s for the monodisperse α,ω-PS$(COOH)_2$ films with M_n of (1) 5.1K, (2) 12K, (3) 52K, and (4) 94K.

In the case of the PS−H, the M_n dependence of T_g^s was more remarkable than that of T_g^b. Characteristic thermal molecular motion at the PS−H surface has been explained in terms of the chain end effect and the reduced cooperativity. The chain end groups of the PS−H are preferentially segregated at the surface due to its lower surface free energy than the main-chain part. Since the chain end groups have the larger freedom than the main-chain part, an excess free volume is induced at the surface. Also, a segment existing at the surface is supposed to have a fewer neighbor segments to move cooperatively owing to the free space on the polymer phase. Thus, active molecular motion takes place at the PS−H surface.

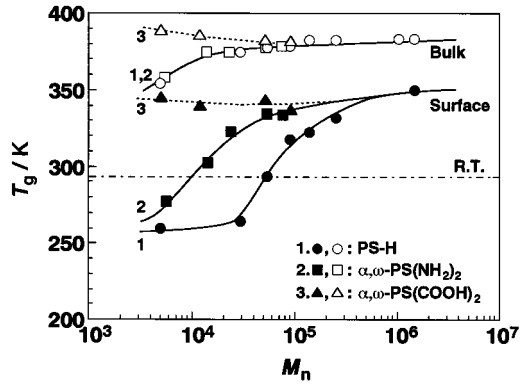

Figure 5. M_n dependences of T_g^s and T_g^b for the PS films with various chain end groups based on SVM and DSC measurements. The filled and open symbols denote T_g^s and T_g^b, respectively.

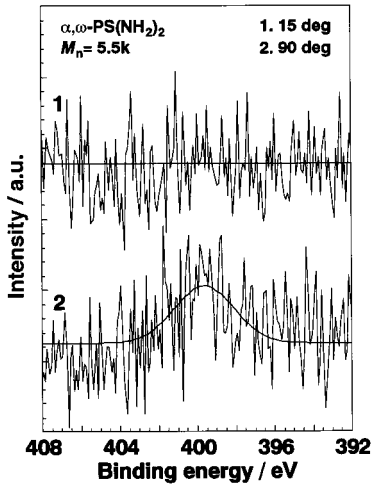

Figure 6. XPS N_{1s} core-level spectra of the α,ω-PS$(NH_2)_2$ film with M_n of 5.5K at emission angle of photoelectrons of (1) 15° and (2) 90°, respectively.

In the case of the α,ω-PS$(NH_2)_2$, the surface free energy of the chain end is relatively larger than that of the main-chain part. Thus, it is inferred that the chain ends are depleted at the surface.[30] To confirm whether it would be true, angular-dependent XPS measurement was carried out. Figure 6 shows the N_{1s} core level spectra of the α,ω-PS$(NH_2)_2$ film at two different emission angles of photoelectron, 15° and 90°. As a sample, α,ω-PS$(NH_2)_2$ with the smaller M_n of 5.5K was used to facilitate the detection of nitrogen atoms due to increasing number density of chain ends. The analytical depth of XPS, d, from the outermost surface is given by

$$d = 3\lambda \sin \theta \qquad (1)$$

where λ is the inelastic mean-free path of photoelectrons in the solid and θ is its emission angle. The analytical depths at $\theta = 15°$ and 90° based on eq 1 were calculated to be 2.7 and 10.5 nm, respectively. At $\theta = 15°$, the N_{1S} signal was not observed at all, as shown in Figure 6. On the contrary, in the case of $\theta = 90°$, the N_{1s} peak was somehow discerned at 400 eV, although the S/N ratio was not necessarily good. Hence, it is plausible that the chain ends of α,ω-PS$(NH_2)_2$ are located at the depth region of 2.7 nm apart from the outermost surface. The indentation depth of a tip in our SVM measurement was estimated to be less than 1 nm based on Johnson−Kendall−Roberts theory.[23] This means that the surface

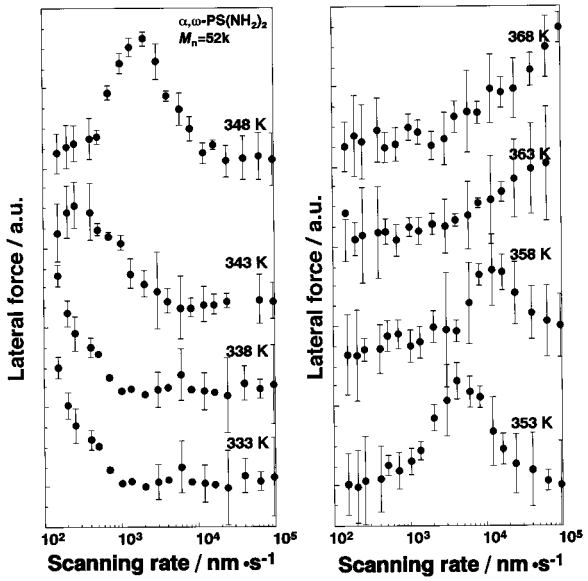

Figure 7. Scanning rate dependence of lateral force for the α,ω-PS$(NH_2)_2$ film with M_n of 52K at the temperature range 333−368 K.

molecular motion of the α,ω-PS$(NH_2)_2$ film evaluated by SVM is not probably affected by chain ends because those are depleted at the surface. Nevertheless, T_g^s was much lower than T_g^b, and the M_n dependence of T_g^s was clear, as shown in Figure 5. Therefore, it seems most likely that thermal molecular motion at the surface is activated by other factors in addition to the chain end effect, such as the reduced cooperativity owing to the existence of the free space on the polymer phase.

In contrast to the PS−H and α,ω-PS$(NH_2)_2$, neither distinct M_n dependence of T_g^s nor T_g^b was observed for the α,ω-PS$(COOH)_2$ film. Since the α,ω-PS$(COOH)_2$ are intermolecularly associated between chain ends via hydrogen bonding,[31] the apparent M_n of the α,ω-PS$(COOH)_2$ increases in comparison with its own M_n.[22] Hence, it is difficult to discuss about the M_n dependence of T_g^s and T_g^b for the α,ω-PS$(COOH)_2$. In any event, it seems reasonable to conclude from Figure 5 that the chain end chemistry is one of the responsible factors determining on the magnitude of T_g^s.

Activation Energy of Surface α_a-Relaxation by LFM. Next, the apparent activation energy of the surface α_a-relaxation was examined on the basis of the time−temperature superposition principle. Since the measuring frequency of our SVM is limited in one decade at present, the complement technique, LFM, was applied to the α,ω-PS$(NH_2)_2$ and α,ω-PS$(COOH)_2$ films. The surface relaxation behavior of the PS−H films has been discussed in detail elsewhere.[23]

Figure 7 shows the scanning rate dependence of lateral force at various temperatures for the α,ω-PS$(NH_2)_2$ film with M_n of 52K. While the lateral force was invariant with the scanning rate at a temperature lower than 323 K (not shown in Figure 7), in the temperature range 333−338 K, the lateral force increased with decreasing scanning rate at the region lower than 10^3 nm s^{-1}. At higher temperatures, 343−358 K, a peak of lateral force was clearly observed, and the peak position was shifted to the higher scanning rate with increasing temperature. Then, the lateral force decreased with a decrease in the scanning rate at the higher temperature than 363 K. Eventually, the lateral force recovered the invariance with respect to the scanning rate (not shown

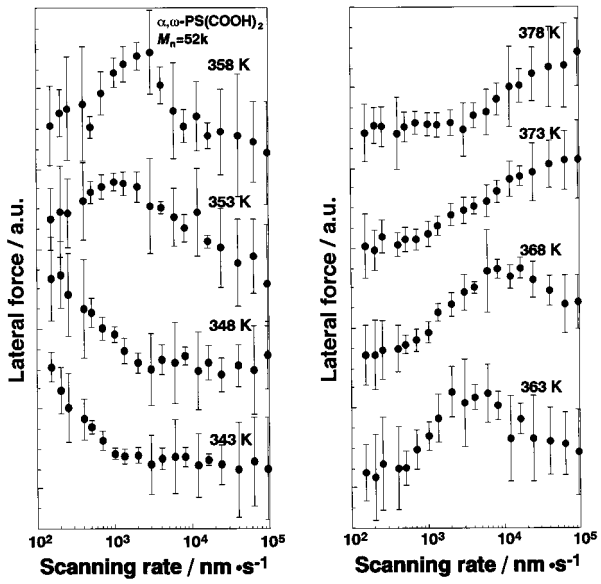

Figure 8. Scanning rate dependence of lateral force for the α,ω-PS(COOH)$_2$ film with M_n of 52K in the temperature range 343−378 K.

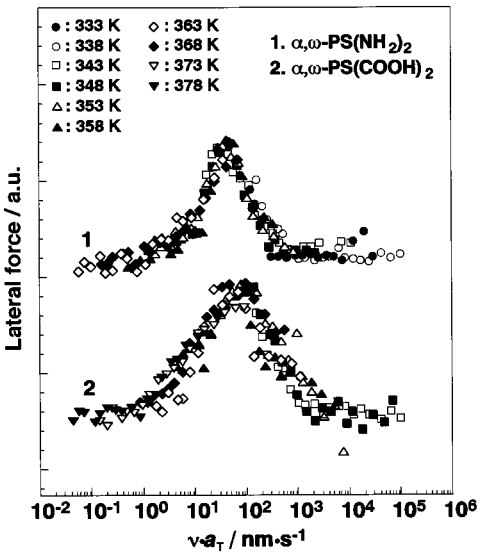

Figure 9. Master curves related to the scanning rate−lateral force relationship for the (1) α,ω-PS(NH$_2$)$_2$ and (2) α,ω-PS(COOH)$_2$ films with M_n of 52K drawn from each curve in Figures 7 and 8. Reference temperatures of 333 and 343 K were used for the α,ω-PS(NH$_2$)$_2$ and α,ω-PS(COOH)$_2$ films with M_n of 52K, respectively.

in Figure 7). Thus, the overall profiles reflect a successive change of the surface molecular motion from the glassy state to the rubbery one via the transition with increasing temperature. Similarly, Figure 8 shows the scanning rate dependence of lateral force as a function of temperature for the α,ω-PS(COOH)$_2$ film with M_n of 52K. The apparent shape change in lateral force−scanning rate curves with increasing temperature for the α,ω-PS(COOH)$_2$ film seems to be the same as that of the α,ω-PS(NH$_2$)$_2$ film, although the relation between the peak position and temperature differs in the two films.

Figure 9 shows the master curves of the lateral force−scanning rate relation for the α,ω-PS(NH$_2$)$_2$ and α,ω-PS(COOH)$_2$ films drawn from horizontal and vertical shifts of each curve shown in Figures 7 and 8 as the

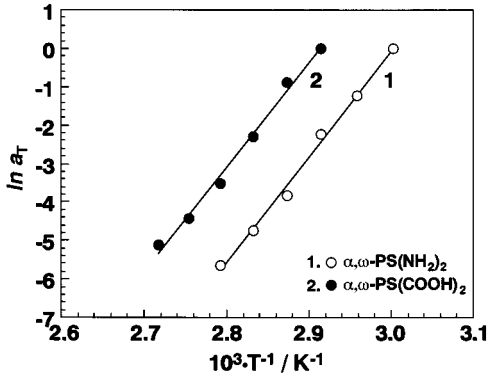

Figure 10. Semilogarithmic plots of shift factor, a_T, vs reciprocal absolute temperature for the (1) α,ω-PS(NH$_2$)$_2$ and (2) α,ω−PS(COOH)$_2$ films with M_n of 52K, respectively.

reference temperatures of 333 and 348 K, respectively. Figure 9 clearly indicates that the time−temperature superposition, which is characteristic of the bulk viscoelastic properties of polymeric materials, can be also applied to the surface α_a-relaxation process of the PS films with hydrophilic chain ends, as already discussed for the PS−H film.[23] Assuming that the relationship between shift factor, a_T, and measuring temperature is Arrhenius type, the apparent activation energy, $\Delta H^{\ddagger}$, of the surface α_a-relaxation process can be calculated from

$$\ln a_T = \frac{\Delta H^{\ddagger}}{R}\left(\frac{1}{T} - \frac{1}{T_0}\right) \qquad (2)$$

where R is the gas constant and T and T_0 are the measuring and reference temperatures, respectively. Figure 10 shows the Arrhenius plots for the α,ω-PS(NH$_2$)$_2$ and α,ω-PS(COOH)$_2$ films. Since the a_T at given temperatures could be unambiguously decided by the horizontal shift in the vicinity of the peak, only six a_T were used to obtain the reliable value of the surface $\Delta H^{\ddagger}$, as shown in Figure 10. The surface $\Delta H^{\ddagger}$ of the α,ω-PS(NH$_2$)$_2$ and α,ω-PS(COOH)$_2$ films so obtained from the line slopes in Figure 10 were 230 ± 10 and 220 ± 10 kJ mol^{-1}, respectively. These values were in good agreement with our previous value of the surface $\Delta H^{\ddagger}$ for the PS−H film, 230 ± 10 kJ mol^{-1}.[23] Hence, it seems likely that the surface $\Delta H^{\ddagger}$ is insensitive to the chemical structure of chain end group. Also, it is noteworthy that the surface $\Delta H^{\ddagger}$ is much smaller than the reported values of the $\Delta H^{\ddagger}$ for bulk samples, ranging from 360 to 880 kJ mol^{-1}.[32,33] The discrepancy of $\Delta H^{\ddagger}$ between at the surface and in the bulk implies that the size and/or energy barrier of the cooperative movement for the α_a-relaxation process are/is reduced at the surface in comparison with the bulk. The reduced cooperativity at the surface can be easily understood by taking into account the fact that the free space is presented to polymer segments at the surface. That is, the existence of the free space induces active micro-Brownian motion at the air/polymer interface. Thus, T_g^s was lower than T_g^b even in the case that the chain end effect can be negligible such as the α,ω-PS(NH$_2$)$_2$, α,ω-PS(COOH)$_2$, and PS−H films with infinite M_n, as shown in Figure 5. Therefore, it is conceivable that the active thermal molecular motion occurs at the surface by the reduced cooperativity in addition to the chain end effect.

Determination Factors on T_g^s. Figure 11 shows the schematic representation of the T_g^s and T_g^b variations

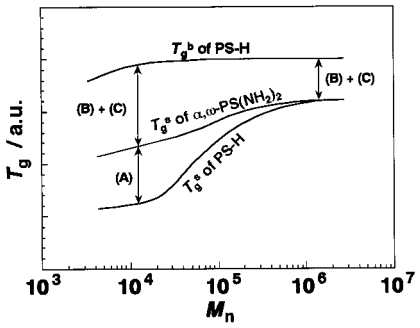

Figure 11. Summary of the determination factors on surface molecular motion for monodisperse PS film. See text for details.

with M_n for the PS−H film as well as the $T_g^s - M_n$ relation for the α,ω-PS$(NH_2)_2$ one. As discussed above, the chain end groups of the PS−H and α,ω-PS$(NH_2)_2$ are enriched and depleted at the surface, respectively. Hence, it seems reasonable to claim that the T_g^s difference between PS−H and α,ω-PS$(NH_2)_2$ might arise from the discrepancy of the free volume fraction related to the surface distribution of chain ends, as shown by (A) in Figure 11. In the case of the infinite M_n, the chain end effect on surface molecular motion is negligible. Nevertheless, it was apparent that T_g^s was lower than T_g^b. This cannot be interpreted by the different free volume fraction induced by the different chain end groups. Thus, it can be envisaged that the difference between T_g^s and T_g^b is in part arisen from the reduced cooperativity for micro-Brownian motion at the surface (B) by virtue of the free space on the polymer phase. Also, the difference between T_g^s of α,ω-PS$(NH_2)_2$ and T_g^b becomes larger with decreasing M_n, as shown in Figure 11. This result suggests that other factor, (C), which should depend strongly on M_n, in addition to (A) and (B) influences on the manifestation of the vigorous thermal molecular motion at the surface. A possible candidate for such a factor is the reduced surface density of chain entanglement[34] and/or extended or oriented chain conformation at the surface.[35] More conclusive works to investigate other factor/s on T_g^s related to surface micro-Brownian motion will be discussed elsewhere.

Conclusion

Glass transition behaviors of the PS−H, α,ω-PS$(NH_2)_2$, and α,ω-PS$(COOH)_2$ films were studied by SVM in conjunction with LFM. It was found that T_g^s was lower than T_g^b even in the case of the α,ω-PS$(NH_2)_2$ and α,ω-PS$(COOH)_2$ films. However, the magnitude of T_g^s was stongly dependent on the chain end chemistry. The surface $\Delta H^{\ddagger}$ of α,ω-PS$(NH_2)_2$ and α,ω-PS$(COOH)_2$ were 230 ± 10 and 220 ± 10 kJ mol^{-1}, respectively. These values were in excellent accordance with the surface $\Delta H^{\ddagger}$ of PS−H and were well below the bulk $\Delta H^{\ddagger}$. Eventually, it was concluded that the peculiar surface molecular motion resulted from chain end effect, reduced cooperativity, and other factors that should have a strong relation to M_n.

Acknowledgment. This work was in part supported by Grant-in-Aids for COE Research (#08CE2005) and Scientific Research (A) (#13355034) from the Ministry of Education, Science, Sports, and Culture and by Research Fellowships of the Japan Society for the Promotion of Science for Young Scientists.

References and Notes

(1) Kajiyama, T.; Tanaka, K.; Takahara, A. *Macromolecules* **1995**, *28*, 3482.
(2) Jean, Y. C.; Zhang, R.; Cao, H.; Yuan, J. P.; Huang, C. M.; Nielsen, B.; Asoka-Kumar, P. *Phys. Rev. B* **1997**, *56*, R8459.
(3) Liu, Y.; Russell, T. P.; Samant, M. G.; Stöhr, J.; Brown, H. R.; Cossy-Favre, A.; Diaz, J. *Macromolecules* **1997**, *30*, 7768.
(4) Schwab, A. D.; Agra, D. M. G.; Kim, J. H.; Kumar, S.; Dhinojwala, A. *Macromolecules* **2000**, *33*, 4903.
(5) Meyers, G. F.; DeKoven, B. M.; Seitz, J. T. *Langmuir* **1992**, *8*, 2330.
(6) Hammerschmidt, J. A.; Gladfelter, W. L.; Haugstad, G. *Macromolecules* **1999**, *32*, 3360.
(7) Fryer, D. S.; Nealey, P. F.; de Pablo, J. J. *Macromolecules* **2000**, *33*, 6439.
(8) Ge, S.; Pu, Y.; Zhang, W.; Rafailovich, M.; Sokolov, J.; Buenviaje, C.; Buckmaster, R.; Overney, R. M. *Phys. Rev. Lett.* **2000**, *85*, 2340.
(9) Tsui, O. K. C.; Wang, X. P.; Ho, J. Y. L.; Ng, T. K.; Xiao, X. *Macromolecules* **2000**, *33*, 4198.
(10) Kerle, T.; Lin, Z.; Kim, H.-C.; Russell, T. P. *Macromolecules* **2001**, *34*, 3484.
(11) Boiko, Y. M.; Prud'homme, R. E. *J. Polym. Sci., Polym. Phys. Ed.* **1998**, *36*, 567.
(12) Rouse, J. H.; Twaddle, P. L.; Ferguson, G. S. *Macromolecules* **1999**, *32*, 1665.
(13) Kawaguchi, D.; Tanaka, K.; Takahara, A. Kajiyama, T. *Macromolecules* **2001**, *34*, 6164.
(14) Keddie, J. L.; Jones, R. A. L.; Cory, R. A. *Europhys. Lett.* **1994**, *27*, 59.
(15) Forrest, J. A.; Dalnoki-Veress, K.; Dutcher, J. R. *Phys. Rev. E* **1997**, *56*, 5705.
(16) DeMaggio, G. B.; Frieze, W. E.; Gidley, D. W.; Zhu M.; Hristov, H. A.; Yee, A. F. *Phys. Rev. Lett.* **1997**, *78*, 1524.
(17) Tseng, K. C.; Turro, N. J.; Durning, C. J. *Phys. Rev. E* **2000**, *61*, 1800.
(18) Kajiyama, T.; Tanaka, K.; Ohki, I.; Ge, S.-R.; Yoon, J.-S.; Takahara, A. *Macromolecules* **1994**, *27*, 7932.
(19) Tanaka, K.; Taura, A.; Ge, S.-R.; Takahara, A.; Kajiyama, T. *Macromolecules* **1996**, *29*, 3040. Kajiyama, T.; Tanaka, K.; Takahara, A. *Macromolecules* **1997**, *30*, 280.
(20) Satomi, N.; Takahara, A.; Kajiyama, T. *Macromolecules* **1999**, *32*, 4474.
(21) Tanaka, K.; Takahara, A.; Kajiyama, T. *Macromolecules* **1997**, *30*, 6626.
(22) Tanaka, K.; Jiang, X.; Nakamura, K.; Takahara, A.; Kajiyama, T.; Ishizone, T.; Hirao, A.; Nakahama, S. *Macromolecules* **1998**, *31*, 5148.
(23) Kajiyama, T.; Tanaka, K.; Satomi, N.; Takahara, A. *Macromolecules* **1998**, *31*, 5150. Tanaka, K.; Takahara, A.; Kajiyama, T. *Macromolecules* **2000**, *33*, 7588.
(24) Doruker, P.; Mattice, W. L. *J. Phys. Chem. B* **1999**, *103*, 178. Jang, J. H.; Ozisik, R.; Mattice, W. L. *Macromolecules* **2000**, *33*, 4271.
(25) Ueda, K.; Hirao, A.; Nakahama, S. *Macromolecules* **1990**, *23*, 939.
(26) Akabori, K.; Tanaka, K.; Takahara, A.; Kajiyama, T. Manuscript in preparation.
(27) Satomi, N.; Tanaka, K.; Takahara, A.; Kajiyama, T. Manuscript in preparation.
(28) Saitô, N.; Okano, K.; Iwayanagi, S.; Hideshima, T. In *Solid State Physics*; Seitz, F., Turnbull, D., Eds.; Academic Press: New York, 1963; Vol. 14, p 343.
(29) In the case of the bulk monodisperse PS−H with M_n of 1.8 M, an onset temperature, at which loss modulus started to increase, was evaluated to be 376 K by the dynamic mechanical analysis using Rheovibron at the frequency of 35 Hz. T_g^b of the same sample determined from the onset temperature of the endothermic baseline shift on the DSC curve was 378 K. See ref 23.
(30) Jalbert, C. J.; Koberstein, J. T.; Balaji, R.; Bhatia, Q.; Salvati, L., Jr.; Yilgor, I. *Macromolecules* **1994**, *27*, 2409. Elman, J. F.; Johs, B. D.; Long, T. E.; Koberstein, J. T. *Macromolecules* **1994**, *27*, 5341.
(31) There is a possibility of hydrogen-bonding formation for the α,ω-PS$(NH_2)_2$ chains. Since T_g^b of the α,ω-PS$(NH_2)_2$ is in good

accordance with the corresponding T_g[b] of the PS−H, however, it seems reasonable to consider that intermolecular association between α,ω-PS$(NH_2)_2$ chains via hydrogen bonding is trivial.

(32) McCrum, N. G.; Read, B. R. *Anelatic and Dielectric Effects in Polymeric Solids*; Dover: New York, 1967; p 414.

(33) Santangelo, P. G.; Roland, C. M. *Macromolecules* **1998**, *31*, 4581.

(34) Brown, H. R.; Russell, T. P. *Macromolecules* **1996**, *29*, 798.

(35) Bitsanis, I. A.; ten Brinke, G. *J. Chem. Phys.* **1993**, *99*, 3100.

MA010126W